http://doi.org/10.15446/ing.investig.87275

Analysis and Discussion of Two-Way Coupling Effects in Particle-Laden Turbulent Channel Flow

Análisis y discusión de los efectos del acople de dos vías en el flujo turbulento de un canal cargado con partículas

Santiago Laín[1], Daniel Ortíz[2], Jesús A. Ramírez[3], and Carlos A. Duque[4]

ABSTRACT

This paper studies the turbulence modification caused by the presence of solid particles in fully developed channel flow by means of the point particle Direct Numerical Simulations (DNS) approach. Inertial particles much smaller than the smallest vortical flow structures are considered, maintaining a volume fraction of the order 10^{-4}, where inter-particle collisions are rare and have nearly no influence on flow development. To avoid concurrent effects that could mask the analysis of fluid-turbulence interaction, gravity is not included in the study, and particle-smooth wall collisions are modelled as ideal reflections. The alteration of fluid turbulence dynamics by the particles is illustrated and discussed, providing an overview of the fluid-particle interaction phenomena occurring at both microscopic and macroscopic flow levels. Finally, the relation of such phenomena with drag-reducing effects by particles is demonstrated.

Keywords: direct numerical simulation, particle-laden channel flow, turbulence, two-way coupling

RESUMEN

Este artículo estudia la modificación de la turbulencia de la fase portadora debido a la presencia de partículas sólidas en un flujo en canal totalmente desarrollado utilizando la aproximación de Simulación Numérica Directa (DNS) con partículas puntuales. Las partículas inerciales consideradas son mucho más pequeñas que la menor de las estructuras vorticales turbulentas, manteniendo una fracción volumétrica del orden de 10^{-4}, en la cual las colisiones entre partículas son esporádicas y apenas tienen influencia en el desarrollo del flujo. Con el fin de evitar efectos simultáneos que puedan enmascarar el análisis de la interacción fluido-partícula, no se incluyen los efectos gravitatorios en el estudio, y las colisiones partícula-pared lisa se modelan como reflexiones ideales. Se ilustra y discute la alteración de la dinámica turbulenta del fluido por parte de las partículas, proporcionando un panorama de los fenómenos de interacción fluido-partícula a nivel microscópico y macroscópico. Finalmente, se muestra la relación de los fenómenos descritos con los efectos de reducción de arrastre causados por las partículas en el flujo en canal.

Palabras clave: simulación numérica directa, flujo bifásico en canal, turbulencia, acoplo de dos vías

Received: May 13th, 2020
Accepted: May 23th, 2022

Introduction

Turbulent flows laden with droplets and particles are commonly found in nature and industrial processes. Examples of the first are sandstorms, clouds, particle sedimentation in rivers and oceans, among others. The evaporation of liquid drops in spray dryers and particle separation in scrubbers or cyclones are examples of the second. Such turbulent dispersed two-phase flows are investigated from both experimental and numerical approaches. This study employs the numerical perspective.

There are three main numerical approaches to such systems (Kuerten, 2016). The most detailed technique is to fully resolve the flow around the particles, whose motion is computed from the external forces and those exchanged with the carrying fluid. This method needs very fine meshes in order to compute the flow around the particles and is usually restricted to handling a small number of particles. This approach is the most adequate for dealing with particles

[1] Physicist, Mathematician, and PhD in Physical Sciences, Universidad of Zaragoza, Spain. Dr.-Ing. Habil. Martin Luther University Halle-Wittenberg, Germany. Affiliation: PAI+ Group, Fluid Mechanics Professor at Universidad Autónoma de Occidente Cali, Colombia. E-mail: slain@uao.edu.co

[2] Mechanical Engineer, Universidad Autónoma de Occidente, Colombia. Affiliation: Projects Engineer, Fundación Universidad del Valle, Colombia. E-mail: danortiz0@gmail.com

[3] Mechanical Engineer and Master in Industrial Maintenance, Universidad Experimental del Táchira, Venezuela; PhD in Mechanical Engineering, Universidad Nacional de Colombia. Affiliation: Professor at Universidad Santo Tomás, Colombia. E-mail: jesusramirez@usantotomas.edu.co

[4] Mechanical Engineer Universidad Nacional de Colombia; Master in Mechanical Engineering, Universidad de los Andes, Colombia; Ph.D. in Mechanical Engineering, University of Warwick, UK. Affiliation: GNUM Group, Professor at Universidad Nacional de Colombia, Colombia. E-mail: caduqued@unal.edu.co

How to cite: Laín, S., Ortíz, D., Ramírez, J. A., and Duque, C. A. (2023). Analysis and discussion of two-way coupling effects in particle-laden turbulent channel flow. *Ingeniería e Investigación, 43*(1), e87275. http://doi.org/10.15446/ing.investig.87275

larger than the Kolmogorov length scale. If particles are sufficiently smaller than such scale, point-mass Lagrangian approaches are usually employed. In them, each particle motion is governed by its own momentum equation, which is based on Newton's second law. Thus, millions of particles can be tracked in the computational domain. In order to deal with dense flows with many large particles, the continuum or Eulerian approaches are employed. In such methods, particles are described by continuous velocity and concentration fields, whose evolution is described by an adequate set of partial differential equations, which has to be solved in addition to the fluid equations (Lain and Aliod, 2000).

In all these numerical approaches, the description of the turbulent dynamics of the fluid can be handled by means of Direct Numerical Simulations (DNS), Large Eddy Simulations (LES), or Reynolds Averaged Navier Stokes (RANS) equations.

This study focuses on Lagrangian point-particle methods in connection with a DNS description of the turbulent flow as applied to a channel flow configuration. The interaction between the two phases (fluid and particles) can be described using different levels of coupling. The simplest approach involves considering that particles move in the fluid field without influencing it at all. This is called *one-way coupling*, and it is appropriate for a very low particle volume fraction α. For higher values, the effect of particles in the flow dynamics cannot be ignored, and the so-called *two-way coupling* (TWC) has to be considered. Finally, if the particle volume fraction is high enough, direct interactions between the particles affect the fluid and particle variables. This is known as *four-way coupling*.

Some relevant previous studies applying Lagrangian point-particle DNS methods in the configuration of channel flow are briefly reviewed herein. The first one-way coupled simulation in a channel flow using DNS with point particles was carried out by McLaughlin (1989). He considered the deposition of aerosol particles in a configuration with a bulk Reynolds number of 2 000, defined using half of the channel height as a length scale. Based on a pseudo-spectral method, Kontomaris *et al*. (1992) conducted a low-resolution DNS study of particle dispersion in a channel with a bulk Reynolds number of around 9 000. A benchmark point-particle DNS with a friction Reynolds number $Re_\tau = 150$ was performed by Marchioli *et al*. (2008). It involved five different groups, each of them with its own numerical code. Small differences were found in the mean velocity profiles, showing noticeable variations in the fluid and particle fluctuating velocities. Moreover, the dispersion of the results was larger regarding the particle concentration profiles in the near-wall region.

According to Elgobashi (1994), one-way coupling is only appropriate for very low particle volume fraction values: $\alpha \leq 10^{-5}$. Therefore, for higher values, the momentum and turbulence modification by the particles cannot be ignored and has to be considered in the fluid equations, including the force exchanged with the particles. Balachandar and Eaton (2010) complemented Elgobashi's classification (1994) by indicating that, when mass loading (defined as the ratio of particle mass to that of the fluid) is of order one or larger, even when α is still small, the effect of particles on carrier phase dynamics should be taken into account. First, research dealt with homogeneous and isotropic turbulence (Boivin *et al*., 1998), where the fluid turbulent kinetic energy and dissipation rate modification by the particles was studied. They identified the role of particle inertia (Stokes number) and mass loading in the decreasing values of both quantities, and they found that small inertia particles increased the turbulent energy spectra, albeit damped by larger inertia particles. Turbulent channel flow laden with particles while including two-way coupling was numerically studied by Pan and Banerjee (1996) with $\alpha \approx 10^{-4}$. These authors found that, for the same value of α, small particles reduced fluid turbulence, but that large particles increased it. The two-way coupled simulations performed by Zhao *et al*. (2010) in a turbulent channel flow with $Re_\tau = 360$ based on the channel height found that the bulk flow velocity was higher in the case with particles than in the particle free flow, which means that drag was reduced. Moreover, they noticed that particles enhanced the fluid Reynolds stress in the stream-wise direction but damped the components in the spam-wise and wall-normal directions. Finally, these authors observed that the velocity streaks were more regular and longer in the particle-laden flow. The constant mass loading two-coupled channel flow simulations performed by Lee and Lee (2015) at $Re_\tau = 180$ aimed to study the effect of the viscous Stokes number (τ^+) in the turbulence modification. They found that, for very low values of $\tau^+ = 0,5$, particles enhanced fluid turbulence, whereas, for $\tau^+ > 5$, it was suppressed by the presence of particles. Two values of $Re_\tau = 150,395$ were studied by Kuerten *et al*. (2011) in a two-coupled particle-laden channel flow, where also heat transfer effects were considered. They reported that particle concentration near the walls was reduced when two-way coupling was considered, a fact explained by the reduction in fluid fluctuating velocity in the wall-normal direction by the particles.

Moreover, a crucial issue that appears in TWC is estimating the fluid velocity at the particle position (Göz *et al*., 2004) because each particle locally modifies such velocity. This fact is also linked to the momentum coupling between phases. The usual approach, based on interpolation schemes and the particle in cell (PIC) method, was able to provide a qualitatively correct interpretation of the particle-fluid interaction in channel flow. However, it has been demonstrated that it suffers from some drawbacks such as a dependence on the number of available particles per computational cell and difficulties in correctly evaluating the fluid velocity at the particle position, since every single particle locally modifies the fluid velocity. In order to improve the estimation of the fluid velocity at particle position, several strategies have been proposed, such as the Force Coupling Method (FCM) by Maxey and Patel (2001), the Pairwise Interaction Extended Point-Particle (PIEP) approach by Akiki *et al*. (2017), or the Exact Regularized Point Particle (ERPP) approach by Gualtieri

et al. (2015). For instance, in wall-bounded flow, Battista et al. (2019) showed that ERPP provided good agreement with experimental results (Righetti and Romano, 2004; Wu et al., 2006; Li et al., 2012). Ireland and Desjardins (2017) also propose a method within the VFEL (volume filtered Euler-Lagrange) framework for estimating the undisturbed fluid velocity at the position of the particle, which provides accurate results in several theoretical limiting cases.

For values of $\alpha > 10^{-3}$, it is agreed that inter-particle interactions cannot be disregarded, since their effects are noticeable in flow development. Four-way coupled simulations of vertical pipe flow were performed by Vreman (2007). This author studied the effect of mass loading, observing that fluid turbulence decreased as mass loading increased. Vreman also realized that wall roughness modelling was the most important effect influencing the results of the particle phase. Other studies (Li et al., 2001; Dritselis and Vlachos, 2008) have found similar results, where the presence of particles suppresses the energy transfer from the span-wise to the transversal (span-wise and wall-normal) directions, enhancing the fluid Reynolds stress anisotropy. Moreover, inter-particle collisions reduce the concentration of particles in the near-wall region, leading to more uniform profiles. In the four-way coupled simulations performed by Vreman (2015) in a channel downward flow at $Re_\tau = 642$, it was found that rough walls improve the turbulence reduction promoted by the particles.

This study considers a particle-laden channel flow at a frictional Reynolds number of 175 and a solid particle volume fraction $\alpha \approx 4\times10^{-4}$. Periodic boundary conditions are applied in both the stream-wise and span-wise directions. The Lagrangian point particle approach is adopted, while the turbulent dynamics of the flow are described by DNS. Variations in the carrier phase variables due to the presence of particles and the modification of the dispersed phase variables given the degree of coupling between the phases are illustrated and discussed.

Summary of the numerical approach

In the particle-laden channel flow, the continuous phase consists of air, which, due to the low velocities considered, can be approximated as an incompressible Newtonian fluid. Therefore, its dynamics are governed by the continuity and Navier-Stokes equations:

$$\nabla \cdot \vec{u} = 0 \tag{1}$$

$$\frac{\partial \vec{u}}{\partial t} + \left(\vec{u}\cdot\nabla\right)\vec{u} = -\frac{1}{\rho}\nabla p + \nu\nabla^2\vec{u} + \vec{F}_p + \prod \delta_{i1} \tag{2}$$

where $\vec{u}$ is the fluid velocity, p the pressure, and ρ,ν are the fluid density and kinematic viscosity, respectively. $\vec{F}_p$ represents the feed-back force that particles exert on the fluid, and $\prod \delta_{i1}$ is the external pressure gradient necessary to keep constant mass flow rate in the channel with periodic boundaries in the stream-wise direction (Capecelatro et al., 2018). The particle motion equation is based on Newton's second law, and its trajectory can be built through the following expressions:

$$\frac{d\vec{x}_{pi}}{dt} = \vec{v}_i \tag{3}$$

$$m_i \frac{d\vec{v}_i}{dt} = \sum \vec{F}_i \tag{4}$$

Here, $\vec{x}_{pi}, \vec{v}_i$ denote the position and velocity of particle i, respectively, m_i is its mass, and $\vec{F}_i$ represents the different forces acting on it. For spherical particles, the Maxey and Riley equation (1983) has been well established; it includes drag, gravity-buoyancy, fluid stress, added mass, and Basset history forces. In this study, solid particles of aluminum are considered, which have a density much higher than the air, and gravity is ignored. Under such conditions, the prevalent contribution is the drag force being the rest of the aforementioned negligible forces (Lain and Sommerfeld, 2007; Sommerfeld and Lain, 2015). In this work, the drag force is written as follows:

$$\vec{F}_{Di} = m_i \frac{\vec{u}_i\left(\vec{x}_{pi}, t\right) - \vec{v}_i}{\tau_i}\left(1 + 0{,}15\, Re_i^{0{,}687}\right) \tag{5}$$

where τ_i is the Stokesian particle relaxation time and Re_i is the particle Reynolds number. Both are defined as

$$\tau_i = \frac{\rho_{pi} d_i^2}{18\rho\nu} \qquad Re_i = \frac{\left|\vec{u}_i\left(\vec{x}_{pi}, t\right) - \vec{v}_i\right| d_i}{\nu} \tag{6}$$

with ρ_{pi}, d_i being the particle density and diameter, respectively.

As the considered particle volume fraction is $\alpha \approx 4\times10^{-4}$, the presence of particles affects the turbulent dynamics of the carrier phase. However, the flow is still dilute enough to neglect the effects of inter-particle collisions (Elghobashi, 1994). Therefore, the action of particles on the fluid phase in Equation (2), $\vec{F}_p$, is computed via the method described by Zhao et al. (2010).

When dealing with turbulent flows constrained by walls, it is customary to work with non-dimensional numbers based on the so-called *wall units*, which are introduced hereafter. The first variables are the kinematic viscosity ν and the friction velocity u_τ, which is defined as:

$$u_\tau = \sqrt{\frac{\tau_w}{\rho}} \tag{7}$$

where τ_w denotes the wall shear stress. With these two variables, scales of length (δ_ν) and time (τ_ν) can be built as follows:

$$\text{Length}\quad \delta_\nu = \frac{\nu}{u_\tau} \qquad \text{Time}\quad \tau_\nu = \frac{\nu}{u_\tau^2} \tag{8}$$

The bulk and friction Reynolds numbers, Re and Re_τ, are defined in terms of the flow bulk velocity U_b and the friction velocity, as follows:

$$Re = \frac{U_b h}{\nu} \qquad Re_\tau = \frac{u_\tau h}{\nu} \tag{9}$$

with h being half of the channel height. Then, the non-dimensional distance to the wall z^+ and the velocity u^+ are expressed as:

$$z^+ = \frac{z u_\tau}{\nu} \qquad u^+ = \frac{u}{u_\tau} \tag{10}$$

Simulation setup

The turbulent flow developed between two infinite parallel walls in a channel, realized by imposing periodic boundary conditions in the stream-wise and span-wise directions. No-slip conditions were imposed at the walls, which were separated by a distance $2h$ along the wall-normal direction. The length of the domain was $2\pi h$ (stream-wise) and πh (span-wise), as per Dritselis and Vlachos (2008). To avoid concurrent effects that could mask the analysis of fluid-turbulence interaction, gravity effects were not included. The Friction Reynolds number was fixed at $Re_\tau = 175$ in this study.

The employed physical properties of the fluid phase were $p = 1,2\ \mathrm{kg/m^3}$ and $\nu = 2\times10^{-5}\ \mathrm{m^2/s}$. The resulting friction velocity of the single-phase flow was $u_\tau = 0,035 m/s$. The semi-height was equal to $175\delta_\nu$, whereas the flow domain comprised $1100\times550\times350$ wall units. Such dimensions were enough to include the expected scales of the largest turbulence structures. The adopted grid resolution was 128^3, and the grid spacing Was uniform in the stream-wise and span-wise directions but stretched in the wall normal direction using a hyperbolic tangent function in the near-wall region. Additionally, the time step employed in the solution of the fluid equations was equal to $0,06\tau_\nu$. Both discretizations (spatial and temporal) were appropriate enough to guarantee reliable DNS results. Continuous phase equations were solved via the finite volume solver Fluent v. 17, employing the following numerical discretization schemes: a third-order scheme MUSCL for the convective, a second-order central scheme for the diffusive terms in space, and the implicit second-order scheme for time. Pressure-velocity coupling was handled by the PISO algorithm.

The flow was initialized with the intrinsically unstable velocity field introduced by Schoppa and Hussain (2002), which has been carefully explained by de Villiers (2006). It consists of imposing stream-wise and span-wise perturbations to the fully developed laminar parabolic profile. This allows fully turbulent conditions of the single-phase flow to be obtained after only 20 flow residence times, defined as $2\pi\mathrm{h}/\mathrm{U_b}$. Once such turbulent flow has reached a statistically steady state, the particles are injected randomly in the flow field. The density and diameter of the particles in this simulation were $\mathrm{p_p} = 2\,700\ \mathrm{kg/m^3}$ and $d = 264\mu m$, respectively, which, in wall units, corresponds to $\mathrm{d^+} = 0,462$ and a relaxation time $\mathrm{T^+} = 27$. The integration of particle motion equations (3) and (4) was performed with a Lagrangian time step around 100 times smaller than that used to solve the fluid equations. The studied particle volume fraction was $\alpha \approx 4\times10^{-4}$ which translates into $1,66\times10^6$ real particles in the flow domain. Moreover, for these conditions, the mass loading was around 0,9. As commented before, such value of α is low enough for inter-particle collision effects to be noticeable, but, together with the resulting mass loading, it is high enough for modulating the flow dynamics. Therefore, additional to the two-way coupled simulation, also a one-way coupled computation, *i.e.*, taking $\vec{F}_p = 0$ in Equation (2), was carried out in this study. In order to focus on the effects produced by fluid-particle interaction on the dynamics of both phases, the influence of gravity was not included, and particle-wall collisions were treated as ideal reflections.

Results

The first step was the validation of the present DNS simulations of the turbulent channel flow. Averaged profiles of the variables were obtained by averaging in time during a period of $2000\tau_\nu$ and then in the homogeneous directions (stream- and span-wise). Thus, the profiles obtained for the mean and rms (root mean square) velocities were compared with the results of Zhao *et al.* (2010), which were obtained in a channel with $Re_\tau = 180$. Figure 1a shows the non-dimensional velocity profile, together with the theoretical linear and logarithmic laws. In Figure 1a, $\mathrm{k} = 0,41$ refers to the von Kármán constant.

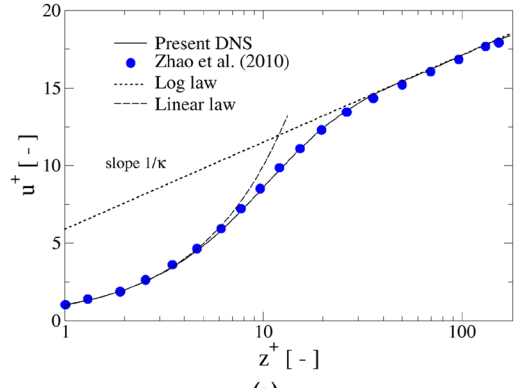

(a)

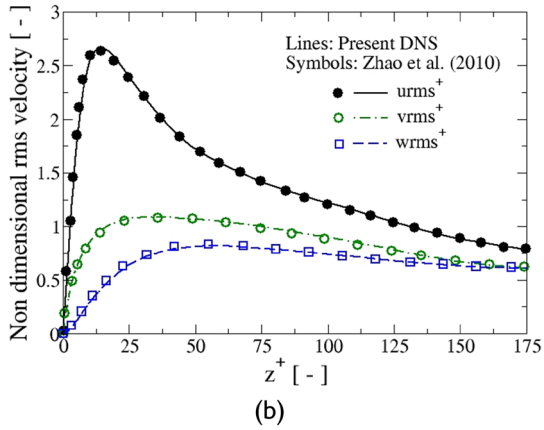

Figure 1. Non-dimensional velocity (a) and rms velocity profiles (b) for the single-phase flow. Comparison with Zhao *et al.* (2010). The theoretical linear and logarithmic laws are also shown in (a).
Source: Authors

Figure 1b shows the behavior of the non-dimensional rms velocities as compared to the results of Zhao *et al.* (2010). It can be seen that the agreement is very good for the mean and fluctuating velocities, which is why the present DNS results can be considered to be validated.

In the first approach, particles can be tracked in the previous flow field under the one-way coupling approach, *i.e.*, disregarding the particle phase influence on the carrier fluid. Afterwards, the effect of particles on the fluid phase is taken into account by the two-way coupling approach. Thus, both degrees of coupling have been performed in the present simulations, which allow describing the effects of two-way coupling between the phases not only on the fluid, but also on the particle phase.

Figure 2 shows the comparison of fluid and particle mean and fluctuating velocities regarding the degree of coupling, *i.e.*, one-way (OWC) or two-way (TWC). Figure 2a presents, in a linear scale, the results for the mean stream-wise velocity made non-dimensional with the single-phase friction velocity. It can be seen that, under two-way coupling, the fluid velocity profile is flatter than in the single-phase flow (SPF), showing two cross-over points: the first one in the buffer layer, $z^+ \approx 20$, where the fluid TWC profiles overcomes the SPF profile; and in the log layer, $z^+ \approx 100$, where the first becomes slower than the second. Such behavior is consistent with the fixed fluid mass flow imposed in the simulations. In the OWC case, particles closely follow the fluid in the viscous

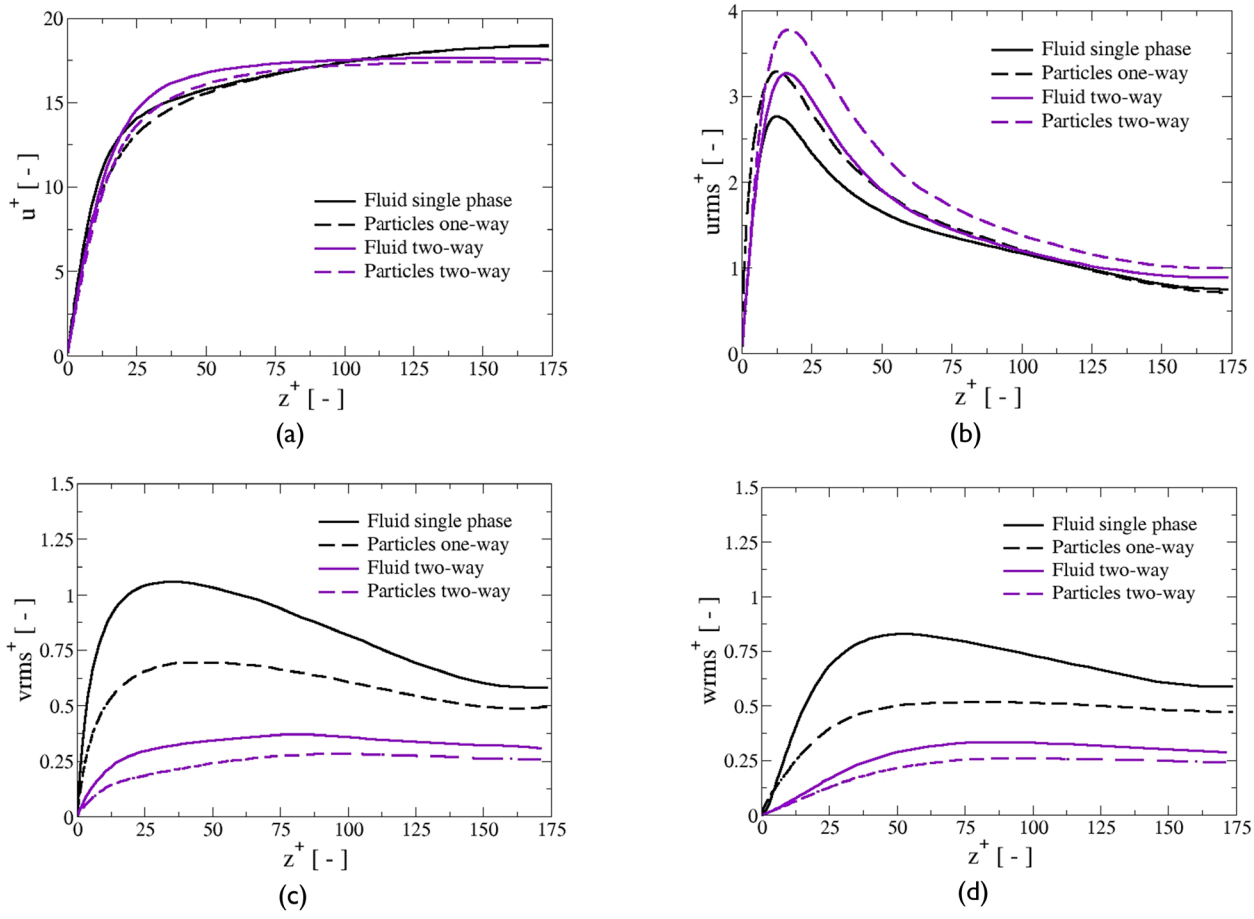

Figure 2. Non-dimensional fluid and particle mean and fluctuating velocities for one-way and two-way coupling conditions: a) stream-wise mean velocity, b) stream-wise rms velocity, (c) span-wise rms velocity, (d) wall-normal rms velocity
Source: Authors

and log layers but lag it in the buffer layer, whereas, in the TWC case, particles always lag the fluid, similar to that reported by Zhao *et al*. (2013).

Figure 2b shows the behavior of the profiles for the stream-wise rms velocity. Consistent with previous literature (*e.g.*, Dritselis and Vlachos, 2008; Zhao *et al*., 2010), the TWC fluid values of this variable are higher than those of the SPF, and the peak value is farther from the wall. The reason for this is that the particle phase, due to its inertia, presents higher values of this variable than the fluid across the whole channel, constituting a source of stream-wise fluctuating velocity for the carrier phase. Furthermore, the particle TWC $urms^+$ values are above those of the particle OWC in the buffer and log layers. On the other hand, the particle OWC profile is above the SPF profile, *i.e.*, up to $z^+ \approx 100$, and then both keep very close values, similar to what happens in the u^+ velocity.

Figures 2c and 2d present the behavior of the non-dimensional span-wise and wall-normal rms velocities, respectively. In both directions, particles are responsible for the strong reduction in the TWC fluid values regarding the SPF all across the channel cross-section, which is again an effect of particle inertia. This phenomenon can be physically explained by the fact that inertial particles tend to maintain their main direction of movement (stream-wise, in this case), not adjusting their velocity to the local flow conditions. In the wall proximity, they keep higher stream-wise velocity fluctuations than the fluid, but the contrary happens in the span-wise and wall-normal directions. Therefore, particles tend to increase fluid stream-wise velocity fluctuations but damp the velocity fluctuations of the other two components. In this way, particles affect the turbulence generation cycle, inhibiting the transfer of energy from the stream-wise to the span-wise and wall-normal directions, which eventually results in an increase in the fluid Reynolds stress anisotropy in TWC. Moreover, in two-way coupling, the near-wall peaks of fluid $vrms^+$ and $wrms^+$ are very much reduced regarding SPF, and those of particles are nearly inexistent. Additionally, it is observed that particle rms values in the span-wise and wall-normal directions are substantially higher in OWC than in TWC. Finally, in TWC, the fluid Reynolds shear stresses are also decreased with regard to SPF (Figure 4b). One last remark is that the obtained non-dimensional profiles of fluid velocity fluctuations in TWC are very close to those presented by Zhao *et al*. (2010).

The analysis of the previous results on velocity profiles cannot disregard the behavior of particle concentration profiles. It is known that, in inhomogeneous turbulent flows, particles tend to migrate to regions with low values of turbulent kinetic energy. This phenomenon has been called *turbophoresis* (Reeks, 1983), and, in the case of near-wall turbulence, it means that particles tend to move towards the wall, accumulating in the viscous sublayer. As a result, particle concentration in the vicinity of the wall can be much higher than at the center of the channel: for instance, in the OWC case shown in Figure 3, such ratio is close to 90. Two-way coupling effects are able to somewhat reduce such value –up to 23 in the TWC results presented in Figure 3 (Lee and Lee, 2015). Particle migration towards the wall depends on particle inertia and reaches a maximum for a certain Stokes number T^+. Obviously, such high particle concentration enhances fluid-particle interactions in the buffer and viscous sublayers regarding the channel center.

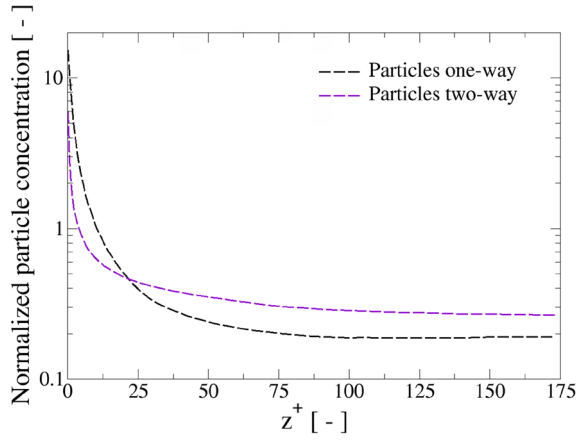

Figure 3. Normalized particle concentration profiles for one-way and two-way coupled simulations
Source: Authors

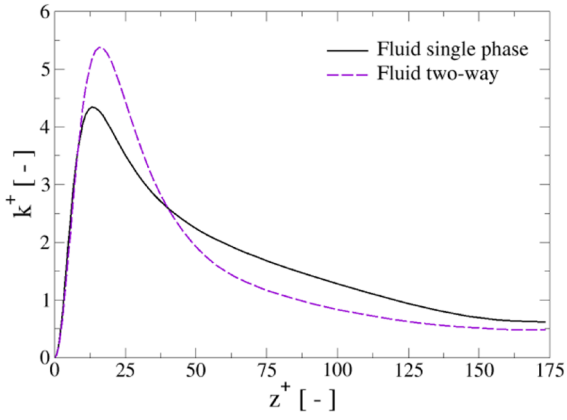

(a)

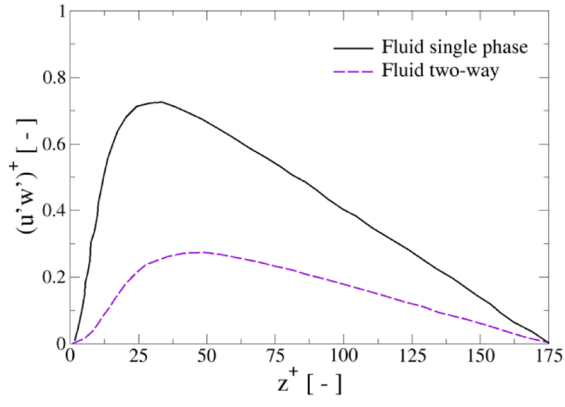

(b)

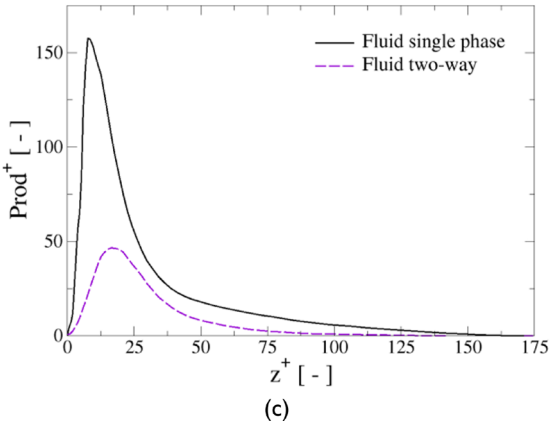

Figure 4. Non-dimensional fluid turbulent kinetic energy (a), turbulent shear stresses (b), and turbulent kinetic energy production term (c) for single phase and two-way coupling conditions
Source: Authors

Except for very small inertia particles very close to tracers, particles tend to laminarize the flow dynamics by decreasing their kinetic turbulent energy, k. Such effect is illustrated in Figure 4, which presents the comparison of the non-dimensional turbulent kinetic energies in SPF and TWC (Figure 4a), together with the profiles for the corresponding Reynolds shear stresses (Figure 4b) and production terms (Figure 4c). The process of reduction of k by the presence of particles can be explained as follows: particles tend to preferentially sample zones with low fluid velocity. This means that the conditionally averaged fluid velocity at particle position tends to be lower than the RANS averaged fluid velocity. As a result, the mean stream-wise slip velocity of particles is negative at the center of the channel but positive in the buffer and viscous layers. This, in turn, means that the fluid provides energy to the particles in the channel core but receives energy from them in the areas close to the wall ($z^+ < 30$). In fact, such energy transfer in the stream-wise direction from the particles to the fluid presents a peak in the buffer layer (Zhang *et al.*, 2013). However, particles dissipate some energy, which is located in the areas with the most presence of particles, *i.e.*, close to the wall due to particles inertia (there is a non-zero slip velocity). Therefore, for the stream-wise direction, the energy extracted from the fluid by particles near the channel center is transferred back to the fluid, mainly in the buffer layer, and part of it is dissipated. Regarding the wall normal and span-wise directions, the energy that particles subtract to the fluid is totally dissipated. As a result, the fluid Reynolds stresses in the stream-wise direction are enhanced regarding the SPF, but they are diminished in the other directions (Figure 2), as well as the Reynolds shear stresses (Figure 4b). In that context, when computing the fluid turbulent kinetic energy, the net result is that, under two-way coupling, it is higher than that of the SPF in the buffer layer but lower in the channel core and viscous regions (Figure 4a). However, because the particles actually dissipate fluctuating energy (Dritselis, 2016), the globally averaged turbulent kinetic energy in the TWC case is lower than that of the SPF, which is actually observed in the present simulations.

Apart of these facts, particles also modulate the fluid turbulence, altering the fluid velocity gradients (mean and fluctuating), which affects the different terms present in the Reynolds stress balance equations. As a consequence, the fluid production under TWC is reduced regarding the SPF (Figure 4c). However, as less turbulent kinetic energy is generated, the fluid dissipation is also reduced. All of these effects are connected with the reduction of velocity-pressure gradient correlations (Dritselis, 2016), which is the mechanism of turbulent energy redistribution among the fluid Reynolds stress components. As a result, in two-way coupled flows, not only is less turbulent kinetic energy produced with regard to the SPF, but its redistribution is also hampered. As consequence, the fluid Reynolds stress anisotropy is enhanced (Figure 2).

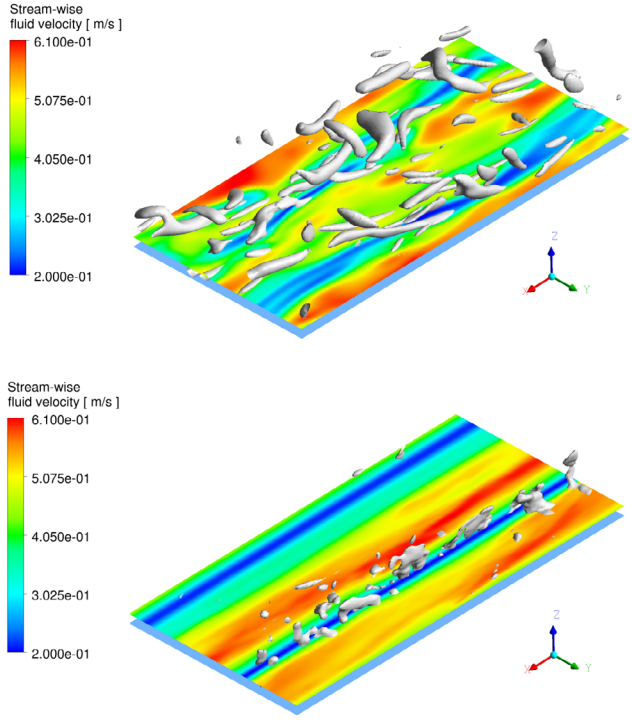

Figure 5. Illustration of the velocity field in the plane $z^+ = 18$ within the buffer layer. The turbulent structures identified by the Q criterion are included. a) Single phase flow, $Q = 50\ s^{-2}$; (b) two-phase flow, $Q = 10\ s^{-2}$. Flow is in the positive x-direction.
Source: Authors

Because of the presence of particles, the main mechanism for the production of k, vortex stretching, is inhibited, a fact that is linked to the damping of vorticity in the stream-wise direction. The consequent decrease in the stream-wise enstrophy (Dritselis, 2016) due to the particles results in a reduction in the number of turbulent structures and their weakening. As an example, Figure 5 shows the turbulent structures visualized by the Q criterion (Hunt *et al.*, 1988) as grey surfaces in single-phase flow (Figure 5a) and in particle-laden flow (Figure 5b). Not only is the number of turbulent structures larger in SPF, but the intensity is also much higher. Figure 4a shows structures with $Q = 50 s^{-2}$, whereas those in Figure 4b have $Q = 10 s^{-2}$.

Another effect of particles on the fluid can also be seen in Figure 5: the length and coherence of the low and high velocity streaks in the buffer layer are increased in TWC with regard to SPF. For instance, in Figure 5, such streaks are shown for a plane located at $z^+ = 18$. In the SPF case (Figure 5a), they are noticeably wavier and shorter than in the TWC configuration (Figure 5b), where they even extend along the whole length of the computational domain. Moreover, particles tend to follow the low velocity streaks more closely than the high velocity streaks, as seen in Figure 6. In this Figure, particle positions are superimposed to the fluid velocity contours in the buffer layer slice of $z^+ = 18$. For both situations –SPF (Figure 6a) and TWC (Figure 6b)– particles are more concentrated in low-speed streaks, forming long elongated ropes, even though it is more evident in TWC. Such concentration stabilizes the low-velocity streaks (making them more inertial) against lateral perturbations, which renders them stabler and straighter (Marchioli, 2003). In the high-speed streaks, there are also particles that are clustered but more dispersed, showing shorter lengths and noticeable voids in both span-wise and stream-wise directions. A very interesting fact is that, especially in TWC, particles clustered in the low-speed streaks escape from the wall (white dots), whereas particles clustered along high-speed streaks are moving towards the wall (black dots).

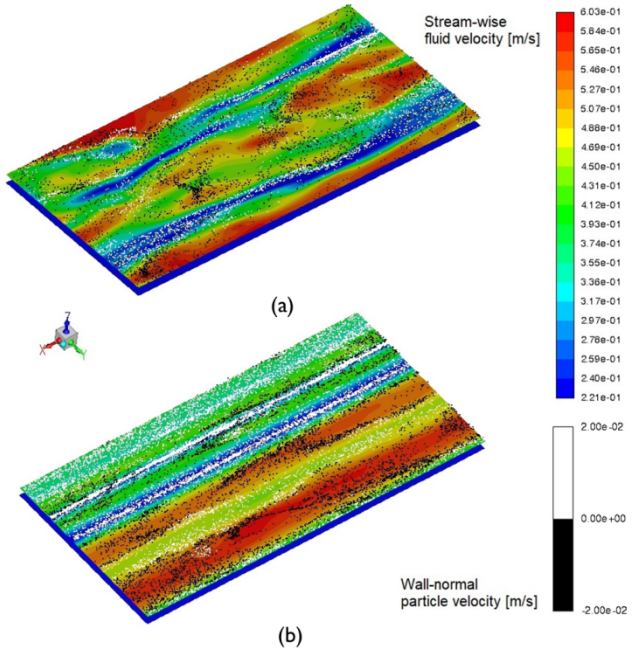

Figure 6. Illustration of the velocity field in the plane $z^+ = 18$ within the buffer layer under one-way coupling (a) and two-way coupling (b) configurations. Positions of particles around that plane are shown as colored dots. Black dots represent particles moving towards the wall, whereas white dots denote particles escaping from the wall. Flow is in the positive x-direction.
Source: Authors

Figure 7 shows the stream-wise velocity field in the middle stream-wise plane. One-way coupled flow (Figure 7a) and two-way coupled flow (Figure 7b) are presented. Moreover, the position of particles is shown as colored dots. Blue and black dots indicate particles with positive and negative wall-normal velocity, respectively. In such plots, the color transition from cyan to yellow is quite fast, indicating a high gradient of stream-wise velocity. Therefore, iso-surfaces of green color can be taken as a boundary among high- and low-speed regions. From Figure 7, it is possible to observe the following facts: 1) particle concentration at the walls is noticeably higher than at the center of the channel; 2) in the channel core, particles are not uniformly distributed, but they concentrate preferentially in clusters, which are more defined in the case of TWC; and 3) particle ejections from the wall are clearly visible thanks to the clustered particles escaping from the wall (blue dots near the lower wall and black dots near the upper wall), where the background color is cyan to green (delimiting the low speed streaks). In OWC, particle ejections are shorter and more compact than in TWC, where they penetrate deeper towards the channel core. Moreover, although it is not shown, there is a strong correlation between wall-normal particle and fluid velocities.

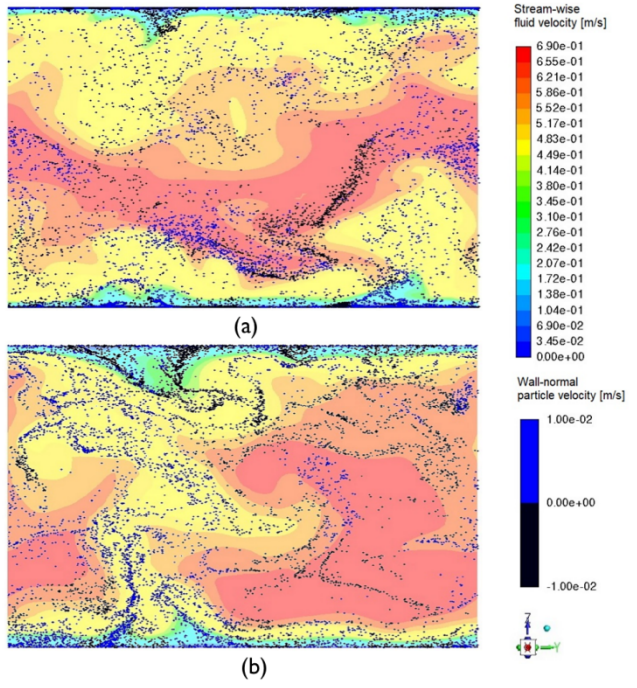

Figure 7. Illustration of the stream-wise velocity field in the middle stream-wise plane under one-way coupling (a) and two-way coupling (b) configurations. Positions of particles around that plane are shown as colored dots. Black dots represent particles with negative wall-normal velocities, whereas blue dots denote particles with positive wall normal velocities. Flow is orthogonal to the plane.
Source: Authors

Discussion

This section aims to pinpoint the main effects of inertial particles on the turbulent behavior of the flow, as well as the mechanisms that drive them. Our aim is to explain the way in which particles interrupt the turbulent generation cycle near the walls. Therefore, the turbulent flow dynamics in the vicinity of a wall are summarized.

According to Jiménez and Pinelli (1999), the self-sustained turbulent regeneration cycle in the near-wall region consists of the formation of sinuous low-velocity streaks from the advection of the mean shear profile by stream-wise vortices. Such streaks, with a typical stream-wise length of 1 000 wall units, are unstable under lateral perturbations. The result of such instability is the generation of quasi stream-wise vortices. In turn, such vortices generate strong coherent motions of fluid that control turbulent mixing near the wall, which are called *sweeps* and *ejections*. The former bring high-speed fluid from the outer flow towards the wall, whereas the latter transport low momentum fluid near the wall to the outer region. Such sweeps and ejections contribute to Reynolds stresses, increasing turbulence production (Marchioli, 2003). Low-speed streaks are longer than the quasi stream-wise vortices (with a typical length of 200 wall units) that generate them and are long-lived structures.

In a near wall particle-laden flow, the solids are driven to the wall by the sweeps and entrained in the outer flow by the ejections. However, as demonstrated by Marchioli (2003), particle exit fluxes are weaker than inlet ones due to the geometrical arrangement of the quasi stream-wise vortices flanking the low-speed streaks. The net result is that particles tend to migrate towards the wall and accumulate in the viscous layer under low-speed streaks –which are mainly related to ejection events (Figure 6)– in regions with low values of wall shear stress. In this context, low speed streaks laden with particles acquire inertia, so their meandering is reduced, which in turn has the effect of inhibiting the instability that generates the quasi stream-wise vortices. Therefore, the tripping frequency of such vortices is decreased, eventually reducing the frequency and intensity of turbulence production events (sweeps and ejections). As a result, turbulence production is diminished in a particle-laden flow.

On the other hand, the degree of turbulence suppression by particles is directly related to particle segregation near the wall, which is enhanced for maximal turbophoresis. In this region, a strong interaction between the concentration of suspended particles and coherent structures is established, thus resulting in weaker near-wall quasi-stream vortices with larger diameters and a longer stream-wise extent than in particle free flow (Dritselis and Vlachos, 2011). Such fainted quasi-stream vortices are not able to produce sweeps and ejections that are energetic enough to sustain the mechanisms of turbulence production at the same rate, and, consequently, turbulent kinetic energy is reduced. The weak intensity of the quasi stream-wise vortices in particle-laden flow also has the effect of reducing the production of coherent vorticity, which, added to the particles' direct effect of decreasing gradients of fluid velocity (Dritselis, 2016), inhibits the mechanisms of turbulence generation (*e.g.*, vortex stretching). As a consequence, the fluid dissipation rate drops accordingly to counterweight the lower turbulent kinetic energy production. Additionally, due to the lower vorticity magnitude, fluid pressure also decreases, with the consequence of lessening the pressure gradient velocity correlations, which are the mechanism responsible for the inter-component turbulent energy exchange. Thus, particles indirectly alter the development of fluid turbulence processes.

Regarding the macroscopic energy flow in the TWC situation, the picture can be summarized as follows: the fluid performs work on the particles in the log layer near the channel center, so they absorb energy from the large eddies and transfer it to the small-scale vorticity structures close to the walls (Zhao *et al.*, 2013). As a result, particles transfer energy to the fluid in the viscous and buffer layers. However, there is an energy imbalance, and the net budget is that particles extract energy from the fluid. Moreover, as commented above, in the vicinity of the wall, inertial particles tend to keep their stream-wise velocity, transferring momentum to the fluid in that direction and extracting momentum from the fluid in the transversal directions. As consequence, the Reynolds stress anisotropy is larger in TWC than in SPF.

From the previous discussion, it seems that particles disturb the near-wall autonomous turbulence regeneration cycle and, in particular, they alter the dynamics of the low velocity streaks, rendering them longer, straighter, and more regular. However, this is a typical characteristic of drag-reduced flows, regardless of the origin of such reduction. Thus, it is not surprising that particle flows laden with particles of certain inertia exhibit reduced drag regarding SPF (Zhao *et al.*, 2010, 2013). In the simulations shown in this work, where the fluid mass flow is fixed, drag reduction should manifest as a reduction in the external pressure gradient necessary to maintain such flow rate (Π in Equation (2). This is indeed the case, and it is shown in Figure 8.

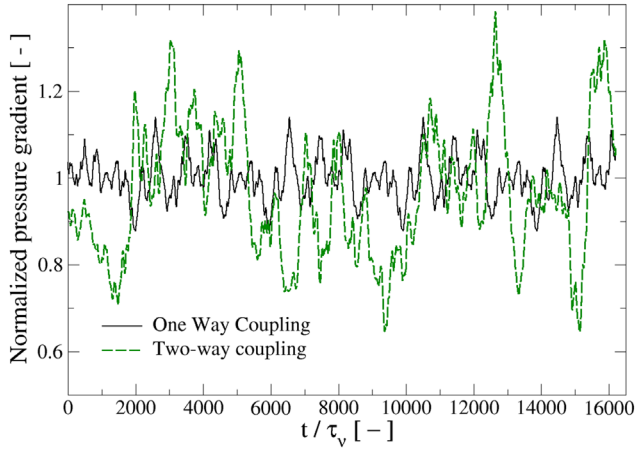

Figure 8. Time evolution of normalized pressure gradient for the one-way and two-way coupling scenarios
Source: Authors

The SPF and TWC external pressure gradient time series are plotted in Figure 8 in non-dimensional form. The pressure gradient is divided by the mean value obtained in

single-phase flow, and time is measured in wall units, *i.e.*, divided by the viscous time scale τ_ν. It can be seen that the fluctuation of the external pressure gradient in TWC flow is much higher than that of SPF. However, when its mean value is computed, it is around 4% lower than that of particle free flow. Finally, it should be mentioned that peaks in the pressure gradient under TWC correspond to bursts of turbulent activity, in which an increase in the number and intensity of turbulent structures can be observed.

Conclusions

This contribution analyzed and discussed the fluid-particle interaction effects that reduce the fluid turbulence intensity in a fully developed two-phase channel flow. Simulations were performed by combining the Direct Numerical Simulation approach and the Lagrangian tracking of point particles including two-way coupling effects. The analysis comprises not only the fluid phase variables, but also the alteration of particle phase variables when two-way coupling interaction is considered in comparison with the one-way coupling approach, *i.e.*, when the momentum feedback from the particles to the fluid is ignored. It has been shown that particles lag the fluid and that the stream-wise fluctuating particle velocity is larger than that of the fluid in the stream-wise direction, albeit lower than that of the fluid in the span-wise and wall-normal directions. Due to their inertia, particles enhance the fluid stream-wise Reynolds stresses but damp the span-wise, wall-normal, and shear stresses. In particular, it was illustrated how particles tend to be segregated in low-velocity streaks, which has the effect of perturbing the autonomous regeneration cycle of wall turbulence, thus reducing the efficiency of turbulence production processes and eventually decreasing the fluid turbulent kinetic energy while laminarizing the flow. Such effects are shown to be responsible for a decrease in the mean pressure gradient, which, in the actual configuration, implies a drag reduction effect by particles in the two-phase channel flow.

Finally, this study provided results coherent with those previously presented in the literature, which allowed presenting a global perspective of the fluid-particle interaction phenomena in the channel flow. Nevertheless, this work has several limitations. In first place, the estimation of the undisturbed fluid velocity at particle position, which is needed in point particle approaches, should be improved by using, for instance, the ERPP method described in Gualtieri *et al*. (2015). On the other hand, including the Saffman force in the particle motion equation is necessary, as it has been demonstrated in the literature (Costa *et al*., 2021). The lift force is responsible for the resuspension of particles close to the wall, causing a reduction in the particle residence time in the low-speed streaks and a diminishing of the particle concentration near the wall. Additionally, when higher particle volume fractions are of interest, inter-particle collisions must be taken into account, as they also contribute to disperse particle ropes located along the fluid streaks, promote decorrelations between fluid and particle velocities, and are a mechanism for energy redistribution among the different components of particle fluctuating velocity, especially in the vicinity of the wall. Finally, in order to approximate real flows, inelastic particle-wall collisions, wall roughness, and particle rotation should be included in the simulation approach. Such effects are to be considered in future simulations.

Acknowledgements

We would like to gratefully acknowledge the support of the Research Directorate of Universidad Autónoma de Occidente and the Research Vice-Principalship of Universidad Nacional de Colombia, through the joint project *Estudio numérico de los procesos de transporte aerodinámico de partículas sólidas en un canal rectangular con rugosidad artificial inducida* [Numerical study of the aerodynamic processes of solid particles in a rectangular channel with induced artificial roughness] (16INTER-264).

References

Akiki, G., Jackson, T. L., and Balachandar, S. (2017). Pairwise interaction extended point-particle model for a random array of monodisperse spheres. *Journal Fluid Mechanics, 813*, 882-928. https://doi.org/10.1017/jfm.2016.877

Balachandar, S., and Eaton, J. K. (2010). Turbulent dispersed multiphase flow. *Annual Review Fluid Mechanics, 42*, 111-133. https://doi.org/10.1146/annurev.fluid.010908.165243

Battista, F., Mollicone, J. P., Gualtieri, P., Messina, R., and Casciola, C.M. (2019). Exact regularised point particle (ERPP) method for particle-laden wall-bounded flows in the two-way coupling regime. *Journal Fluid Mechanics, 878*, 420-444. https://doi.org/10.1017/jfm.2019.622

Bernard, P. S., Ashmawey, M. F., and Handler, R. A. (1989). An analysis of particle trajectories in computer-simulated turbulence channel flow. *Physics of Fluids A, 1*, 1532-1540. https://doi.org/10.1063/1.857330

Boivin, M., Simonin, O., and Squires, K. D. (1998). Direct numerical simulation of turbulence modulation by particles in isotropic turbulence. *Journal Fluid Mechanics, 375*, 235-263. https://doi.org/10.1017/S0022112098002821

Capecelatro, J., Desjardins, O., and Fox, R. O. (2018). On the transition between turbulence regimes in particle-laden channel flows. *Journal Fluid Mechanics, 845*, 499-519. https://doi.org/10.1017/jfm.2018.259

Costa, P., Brandt, L., and Picano, F. (2021). Near-wall turbulence modulation by small inertial particles. *Journal Fluid Mechanics, 922*, A9. https://doi.org/10.1017/jfm.2021.507

de Villiers, E. (2006). *The potential of Large Eddy Simulation for the modeling of wall bounded flows* [Doctoral thesis, Imperial College of Science, Technology, and Medicine] https://scirp.org/reference/ReferencesPapers.aspx?ReferenceID=2169716

Dritselis, C., and Vlachos, N. S. (2008). Numerical study of educed coherent structures in the near-wall region of a particle-laden channel flow. *Physics of Fluids, 20*, 055103. https://doi.org/10.1063/1.2919108

Dritselis, C., and Vlachos, N.S. (2011). Numerical investigation of momentum exchange between particles and coherent structures in low Re turbulent channel flow. *Physics of Fluids, 23*, 025103. https://doi.org/10.1063/1.3553292

Dritselis, C. (2016). Direct numerical simulation of particle laden turbulent channel flows with two- and four-way coupling effects: budgets of Reynolds stress and streamwise enstrophy. *Fluid Dynamics Research, 48*, 015507. https://doi.org/10.1088/0169-5983/48/1/015507

Elghobashi, S. (1994). On predicting particle-laden turbulent flows. *Applied Scientific Research, 52*, 309-329. https://doi.org/10.1007/BF00936835

Göz, M. F., Laín, S., and Sommerfeld, M. (2004). Study of the numerical instabilities in Lagrangian Tracking of bubbles and particles in two-phase flow. *Computers and Chemical Engineering*, 28, 2727-2733. https://doi.org/10.1016/j.compchemeng.2004.07.035

Gualtieri, P., Picano, F., Sardina, G., and Casciola, C.M. (2015). Exact regularized point particle method for multiphase flows in the two-way coupling regime. *Journal Fluid Mechanics, 773,* 520-561. https://doi.org/10.1017/jfm.2015.258

Hunt, J. C. R., Wray, A. A., and Moin, P. (1988). Eddies, streams, and convergence zones in turbulent flows. In Center for Turbulence Research (Eds.), *Proceedings of the Summer Program 1988* (pp. 193-208). https://web.stanford.edu/group/ctr/Summer/201306111537.pdf

Ireland, P. J., and Desjardins, O. (2017). Improving particle drag predictions in Euler–Lagrange simulations with two-way coupling. *Journal Computational Physics, 338*, 405-430. https://doi.org/10.1016/j.jcp.2017.02.070

Jiménez, J., and Pinelli, A. (1999). The autonomous cycle of near-wall turbulence. *Journal Fluid Mechanics, 389*, 335-359. https://doi.org/10.1017/S0022112099005066

Kontomaris, K., Hanratty, T. J., and McLaughlin, J. B. (1992). An algorithm for tracking fluid particles in a spectral simulation of turbulent channel flow. *Journal Computational Physics, 103*, 231-242. https://doi.org/10.1016/0021-9991(92)90398-I

Kuerten, J. G. M., van der Geld, C. W. M., and Geurts, B. J. (2011). Turbulence modification and heat transfer enhancement by inertial particles in turbulent channel flow. *Physics of Fluids, 23*, 123301. https://doi.org/10.1063/1.3663308

Kuerten, J. G. M. (2016). Point-particle DNS and LES of particle-laden turbulent flow – A state-of-the-art review. *Flow, Turbulence and Combustion, 97*, 689-713. https://doi.org/10.1007/s10494-016-9765-y

Laín, S., and Aliod, R. (2000). Study on the Eulerian dispersed phase equations in non-uniform turbulent two-phase flows: Discussion and comparison with experiments. *International Journal of Heat and Fluid Flow, 21*, 374-380. https://doi.org/10.1016/S0142-727X(00)00023-0

Laín, S., and Sommerfeld, M. (2007). A study of pneumatic conveying of non-spherical particles in a turbulent horizontal channel flow. *Brazilian Journal of Chemical Engineering, 24*, 535-546.

Lee, J., and Lee, C. (2015). Modification of particle-laden near-wall turbulence; effect of Stokes number. *Physics of Fluids, 27*, 023303. https://doi.org/10.1063/1.4908277

Li, Y., McLaughlin, J. B., Kontomaris, K., and Portela, L. (2001). Numerical simulation of particle-laden turbulent channel flow. *Physics of Fluids, 13*, 2957-2967. https://doi.org/10.1063/1.1396846

Li, J., Wang, H., Liu, Z., Chen, S., and Zheng, C. (2012). An experimental study on turbulence modification in the near-wall boundary layer of a dilute gas-particle channel flow. *Experiments in Fluids, 53*, 1385-1403. https://doi.org/10.1007/s00348-012-1364-7

Marchioli, C. (2003). *Mechanisms for transfer, segregation and deposition of heavy particles in turbulent boundary layers* [Doctoral thesis, University of Udine] http://calliope.dem.uniud.it/PEOPLE/cris.html

Marchioli, C., Soldati, A., Kuerten, J. G. M., Arcen, B., Tanière, A., Goldensoph, G., Squires, K. D., Cargnelutti, M. F., and Portela, L. M. (2008). Statistics of particle dispersion in direct numerical simulations of wall bounded turbulence: Results of an international collaborative benchmark test. *International Journal of Multiphase Flow, 34*(9), 879-893. https://doi.org/10.1016/j.ijmultiphaseflow.2008.01.009

Maxey, M. R., and Patel, B. K. (2001). Localized force representations for particles sedimenting in Stokes flow. *International Journal of Multiphase Flow, 27*, 1603-1626. https://doi.org/10.1016/S0301-9322(01)00014-3

Maxey, M. R., and Riley, J. J. (1983). Equation of motion for a small rigid sphere in a nonuniform flow. *Physics of Fluids, 26*, 883-889. https://doi.org/10.1063/1.864230

McLaughlin, J.B. (1989). Aerosol particle deposition in numerically simulated channel flow. *Physics of Fluids A, 1*, 1211-1224. https://doi.org/10.1063/1.857344

Pan, Y., and Banerjee, S. (1996). Numerical simulation of particle interactions with wall turbulence. *Physics of Fluids, 8*, 2733-2755. https://doi.org/10.1063/1.869059

Reeks, M. W. (1983). The transport of discrete particles in inhomogeneous turbulence. *Journal of Aerosol Science, 14*, 729-739. https://doi.org/10.1016/0021-8502(83)90055-1

Righetti, M., and Romano, G. P. (2004). Particle–fluid interactions in a plane near-wall turbulent flow. *Journal Fluid Mechanics*. https://doi.org/10.1017/S0022112004008304

Schoppa, W., and Hussain, F. (2002). Coherent structure generation in near-wall turbulence. *Journal of Fluid Mechanics, 453*, 57-108. https://doi.org/10.1017/S002211200100667X

Sommerfeld, M., and Laín, S. (2015). Parameters influencing dilute-phase pneumatic conveying through pipe systems: A computational study by the Euler/Lagrange approach. *Canadian Journal of Chemical Engineering, 93*, 1-17. https://doi.org/10.1002/cjce.22105

Vreman, A. W. (2007). Turbulence characteristics of particle-laden pipe flow. *Journal Fluid Mechanics, 584*, 235-279. https://doi.org/10.1017/S0022112007006556

Vreman, A. W. (2015). Turbulence attenuation in particle-laden flow in smooth and rough channels. *Journal Fluid Mechanics, 773*, 103-136. https://doi.org/10.1017/jfm.2015.208

Wu, Y., Wang, H., Liu, Z., Li, J., Zhang, L., and Zheng, C. (2006). Experimental investigation on turbulence modification in a horizontal channel flow at relatively low mass loading. *Acta Mechanica Sinica, 22*, 99-108. https://doi.org/10.1007/s10409-006-0103-9

Zhao, L. H., Andersson, H. I., and Gillissen, J. J. J. (2010). Turbulence modulation and drag reduction by spherical particles. *Physics of Fluids, 22*, 081702. https://doi.org/10.1063/1.3478308

Zhao, L. H., Andersson, H. I., and Gillissen, J. J. J. (2013). Interphasial energy transfer and particle dissipation in particle-laden wall turbulence. *Journal Fluid Mechanics, 715*, 32-59. https://doi.org/10.1017/jfm.2012.492